3

Signatures of tsunami in the coastal landscape

INTRODUCTION

Tsunami are high-magnitude phenomena that can achieve flow velocities at shore of $15\,m\,s^{-1}$ or more. These flows have the potential to leave many depositional and erosional signatures near the coastline (Figure 3.1). Dawson *et al.* (1991), Dawson and Shi (2000) have attempted to catalog some of these signatures, but ignore bedrock erosional and large-scale landscape features. Figure 3.2 rectifies these deficiencies by encompassing most of the geomorphic signatures found in the literature. The impact of paleo-tsunami can be identified where these signatures have been preserved, either singly or in combination. The depositional signatures of tsunami can be further subdivided into sedimentary deposits and geomorphic forms. The most commonly recognized depositional signature is the occurrence of anomalous sand sheets or lamina sandwiched in peats or muds on coastal plains. The sedimentary deposits, except for imbricated boulders, are less dramatic because they do not form prominent features in the landscape. Without detailed examination, they also could be attributed to other processes. Many of the signatures, such as aligned stacks of boulders, also reveal the direction of approach of a tsunami to a coastline. In many cases, tsunami have approached at an angle to the coast—a feature not commonly associated with the dynamics of tsunami described in Chapter 2. Suites of signatures define unique tsunami-dominated coastal landscapes. The signatures of tsunami will be described in this chapter, while the formation of tsunami-generated landscapes will be discussed in Chapter 4.

The signatures of tsunami were formulated from field evidence linked to earthquake-generated tsunami around the Pacific Rim and to the presence of tsunami identified along a 400 km stretch of the south coast of New South Wales, Australia (Figure 3.3a). Many of the features summarized in Figure 3.2 are dramatic and allude to tsunami events an order of magnitude larger than those normally associated with earthquake-generated tsunami. These latter types of signatures have since been used

Figure 3.1. The remnant plug at the center of a vortex bored into granite at the front of a cliff at Cape Woolamai, Phillip Island, Victoria, Australia. The ridges in the foreground indicate that flow around the plug was counterclockwise and consisted of a double helix. A catastrophic tsunami wave produced the vortex as it washed along the cliff. See color section. © John Meier.

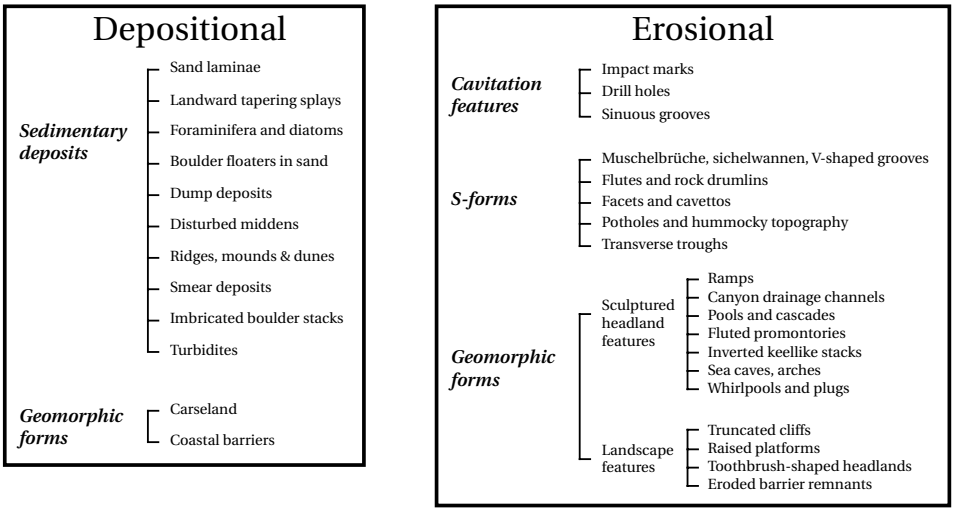

Figure 3.2. Depositional and erosional signatures of tsunami.

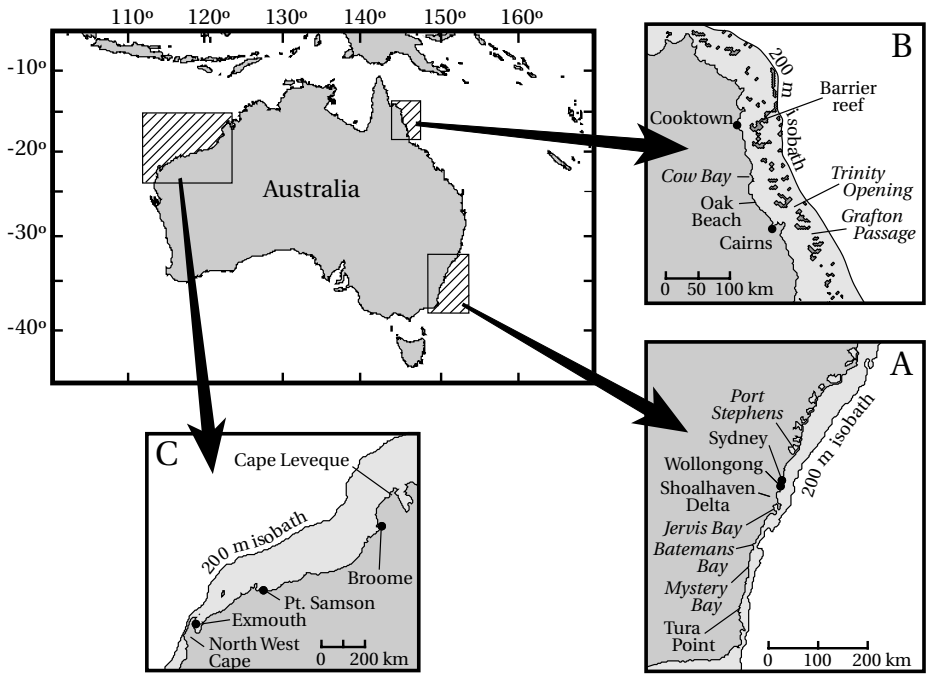

Figure 3.3. Locations of coastline around Australia showing the most prominent signatures of paleo-tsunami: (A) south coast of New South Wales, (B) Cairns Coast, northeast Queensland, and (C) northwest West Australia.

to identify the presence of paleo-tsunami along other sections of the Australian coastline, particularly in northeastern Queensland, northwest Australia, and on Lord Howe Island in the Tasman Sea, and in New Zealand, and along the east coast of Scotland. It is not intended here to debate the merits of this evidence, as this has been done in many peer-reviewed scientific papers. The signatures of large tsunami are not related to storms. Submarine landslides, asteroid impacts with the ocean, and the largest earthquakes produce mega-tsunami features. This evidence will be presented in Part III of this book.

DEPOSITIONAL SIGNATURES OF TSUNAMI

Buried sand or anomalous sediment layers

(Atwater 1987; Dawson, Long, and Smith, 1988; Darienzo and Peterson, 1990; Dawson *et al*., 1991; Minoura and Nakaya, 1991; Clague and Bobrowsky, 1994; Dawson, 1994; Minoura, Nakaya, and Uchida, 1994; Pinegina *et al*., 1996)

The commonest signature of tsunami is the deposition of landward-tapering sandy units up to 50 cm thick sandwiched between finer material and peats on flat coastal

plains. While similar lenses can be deposited by individual surging waves during tropical cyclones, such units are rarely longer than 10 m–20 m and do not form continuous deposits behind modern beaches. Tsunami sand units form part of a coherent landward thinning splay of fining sediment extending up to 10 km or more inland. The thickness of laminae decreases landward while that of an individual unit decreases upward, implying waning energy conditions. All these characteristics match transport of sediment-rich flows by tsunami across marsh surfaces. Tsunami can also deposit discontinuous pencil-thin lenses or wavy wisps of silt in a matrix of much finer material. Thicker units are characterized by a series of fining upward sequences stacked one upon each other. Each unit appears to be indicative of a single wave in the tsunami wave train, although these are indistinguishable from each other without detailed sedimentological analysis. Anomalous sand layers can have an erosional basal contact and incorporate rip-up clasts of muddier sediment. Where they are deposited over water-saturated sediment, the layers may press into the underlying surface, producing loading structures that can be preserved in the stratigraphic record. The layers can also contain shell- and land-based plant material such as twigs and leaves. This material is deposited toward the top of the unit, where it eventually decays into a humic-rich layer.

The coarsest sediment transported in suspension by a wave is deposited first as the wave's velocity slackens inland. This is followed by deposition of ever-decreasing grain sizes. The upper surface of the deposit may be truncated by backwash. However, because backwash is more likely to be channelized, truncation probably occurs as the next wave sweeps across a previously deposited sand unit. The coarsest unit in a deposit usually represents the biggest wave in the wave train. Thus, the relative size of sediment in each unit gives an indication of the relative magnitude of each wave. The number of units is often characteristic of the causative mechanism of the wave. For example, tsunami generated by submarine landslides generally produce wave trains with two to five large waves. Each wave is capable of moving sediment inland. Multiple sand layers cannot be produced by storm surge because it occurs as a single wave event. In contrast, earthquake-generated wave trains, while consisting of tens of waves, tend to produce only a single wave that is large enough to transport sediment inland. Without additional evidence, it may be difficult to separate an earthquake-generated tsunami deposit from that produced by a storm surge.

Figure 3.4 shows the relative grain size and sorting in a 52 cm thick sand unit at Ardmore, Scotland, deposited by large tsunami from the Storegga slide off the west coast of Norway 7,950 years ago. This tsunami deposited fine sand and silt as much as 80 km inland across numerous estuarine flats—termed carseland—that are now raised along the east coast of Scotland. The tsunami and its wider impact will be described in more detail in Chapter 6. Each wave in Figure 3.4 is numbered sequentially. The first wave, as expected, had the greatest wave energy and moved a greater range of grain sizes. Subsequent waves moved finer sediment, probably because of decreasing wave height or availability of coarser sediment. While the last wave was smaller, it transported a wider range of grain sizes than the previous three waves. This may reflect the recycling of coarse sediment seaward by channelized backwash.

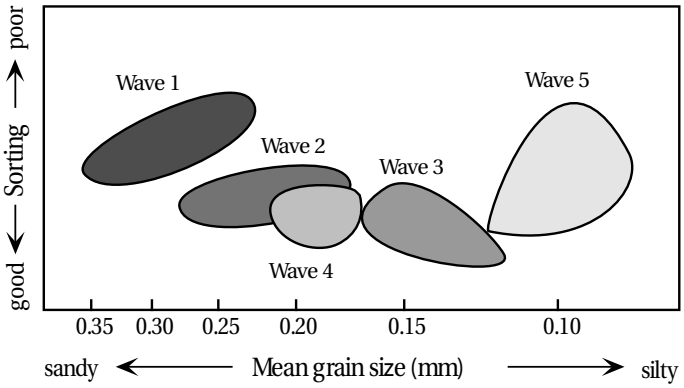

Figure 3.4. Grain size and sorting relationships throughout a 52 cm thick sand unit at Ardmore, Scotland, deposited by a tsunami associated with the Storegga submarine slide.

Sediment layers have been deposited by numerous historical tsunami. The November 1, 1755 Lisbon tsunami, generated by one of the largest earthquakes ever, deposited sand layers along the Portuguese coast and as far as the Isles of Scilly off the west coast of England. In the 20th century, the Grand Banks tsunami of November 18, 1929, which was produced by a submarine landslide, laid down sand layers on the Burin Peninsula in Newfoundland. Following the Chilean tsunami of May 22, 1960, sand layers were deposited in the Río Lingue estuary of south–central Chile, while the Alaskan tsunami of March 27, 1964 deposited sand units along the coasts of British Columbia and Kodiak Island. More recently, this signature was observed on the island of Flores, Indonesia, following the tsunami of December 12, 1992 and along the Aitape coast, Papua New Guinea, as the result of the tsunami of July 17, 1998. In both of the latter cases, landward-tapering wedges of sand were deposited over 500 m inland from the shoreline. These examples will be described in more detail in Chapter 5.

Sand units also allude to paleo-tsunami. For example, a sand unit was deposited by a tsunami within clayey estuarine sediment, up to 10 km inland, on the Shoalhaven delta in southeastern New South Wales 4,700–5,100 years ago. The source of this event is most likely attributable to an asteroid impact in the Tasman Sea. Considerable attempts have been made to date anomalous sand layers and relate them to historical tsunami events. However, because tsunami events occur so infrequently along many coasts, the true value of such dating programs lies in the delineation of the recurrence interval of such a hazard, especially along coastlines that have only been settled in the last few centuries. For example, on the southeastern coast of the Kamchatka Peninsula of eastern Russia, sand layers are preserved in peats or organic-rich alluvium. These sequences also contain volcanic ash layers or tephras that can be used to date the sequences. The tsunamigenic layers consist of coarse marine sand mixed with gravel and pebbles in landward-tapering sheets 2 cm–3 cm thick. The largest tsunami overrode terraces 15 m–30 m above sea level up to 10 km from the coast. Many of the layers show evidence of suspension transport of

sediment, in some cases aided by the passage of tsunami over frozen or icy ground. Forty events can be identified over the past 2,000 years, revealing a recurrence interval of one major event every 50 years. Not all events, though, may have been preserved, because the recurrence interval since 1737 averages one tsunami event every 12.3 years.

In northern Japan rhythmic sedimentary units, consisting of coarsening-upward sequences lying unconformably on top of each other, have been found in lagoons, and linked to historical tsunami over the last 250 years. In a back barrier lagoon at Lake Jusan on the northern end of Honshu Island, facing the Sea of Japan, thicker layers of medium sand 40 cm or more in thickness are sandwiched within organic ooze. Sedimentological analysis indicates that the sands originated from sand dunes or the open ocean beaches. These deposits have been linked to large tsunami events with wave heights in excess of 6 meters occurring at intervals of 250–400 years over the past 1,800 years. On the Pacific coast of Honshu, on the Sendai Plain, as many as five sand layers are sandwiched in peats up to 4 km inland. Two of the upper layers can be correlated to killer tsunami that swept over the plain in 869 and 1611. Along the Sanriku coast of northeast Honshu Island—renowned for deadly tsunami—up to 113 well-sorted sand layers can be found intercalated within black organic muds in swamps and ponds. The sand layers are spatially extensive but do not form erosional contacts with the underlying muds. This suggests that sediment settled from suspension in quiescent waters stranded in depressions after rapid drowning by tsunami that exceeded 1 m in height. The layers have been correlated to known tsunami events originating off the coast and from distant sources in the Pacific Ocean (Table 3.1). Seven of the tsunami formed locally; however, four of the events originated from either Chile or the Kuril Islands to the north. Surprisingly, the severe Chilean tsunami of May 22, 1960 did not flood any of the marshes. In addition, no event prior to 1710 is preserved in the sediments despite this coastline having historical records of earlier events. The stratigraphic evidence designates this coastline as the most frequently threatened inhabited coastline in the world.

Along the west coast of North America, the sand layers are trapped within peats, show sharp non-erosional upper contacts, and erosional bottom ones. The sand layers are 1 cm–30 cm thick (Figure 3.5) and similar in grain size to beach and dune sands on the adjacent seaward coast. Both optical luminescence dating of quartz sand and radiocarbon dating of buried carbon indicate that a great earthquake occurred along 700 km of the Cascadia subduction zone 300 years ago. The exact age has been inferred from the recording of a tsunami in Japan on January 26, 1700. The Kwenaitchechat North American Indian legend in Chapter 1 referred to this event. At least five other events have been identified, with three of the largest occurring somewhere between 600 and 900; 1,000 and 1,400; and 2,800 and 3,200 years ago. At Crescent City, California, up to 12 additional sand layers have been found in a peat bog. This record is similar to the Kamchatka Peninsula in frequency. Interestingly, the tsunami from the Great Alaskan Earthquake of March 27, 1964 only produced a thin sand layer about a centimeter thick here. The lack of cross-bedding in the units indicates deposition out of turbulent suspension, while alteration within the same unit between sand and silty clay suggests pulses of sediment entrainment, transport,

Table 3.1. Correspondence between the inferred age of anomalous sand layers and dated tsunami events on the Sanriku Coast of northeast Honshu Island, Japan.

Inferred age	*Closest corresponding event*	*Source*
1948	March 4, 1952	Hokkaido
1930	March 3, 1933	Sanriku
1905	June 5, 1896	Sanriku
1887	May 9, 1877	Chile
1861	August 13, 1868	Chile
1853	July 23, 1856	Sanriku
1843	July 20, 1835	Sanriku
1805	January 7, 1793	Sanriku
1787	June 29, 1780	Kuril Islands
1772	December 16, 1763	Sanriku
1769	March 15, 1763	Sanriku
1742	May 25, 1751	Chile
1710	July 8, 1730	Chile

Source: From Minoura, Nakaya, and Uchida (1994).

and deposition. Storm waves or surges can be ruled out as mechanisms of emplacement because most of the sites have a high degree of protection from the open ocean.

By far the thickest sand layers were deposited by the recent Indian Ocean Tsunami of December 26, 2004. In Banda Aceh, Indonesia, the sand layer was a massive 0.7 m thick and contained angular pebbles and soil rip-up clasts. In Sri Lanka, the sand layer was 0.37 m thick. This event will be described in detail in Chapter 5.

Foraminifera and diatoms

(Dawson *et al.*, 1996; Dawson, 1999; Haslett, Bryant, and Curr, 2000)

Silty sand units deposited inland by tsunami can also contain a distinct signature of marine diatoms or foraminifera. Foraminifera are small unicellular animals, usually about the size of a grain of sand, that secrete a calcium carbonate shell. On the other hand, diatoms are similarly sized, single-celled plants that secrete a shell made of silica. Both organisms vary in size and live suspended either in the water column (planktonic) or on the seabed (benthic). Under fair-weather conditions, only the larger benthonic species are transported shoreward as bedload under wave action

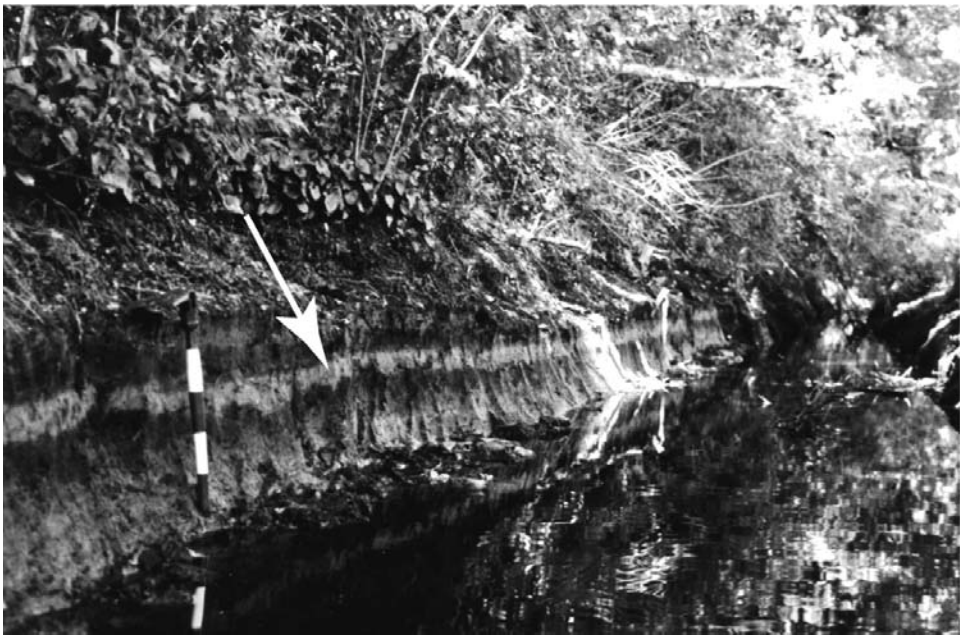

Figure 3.5. Sand layer, deposited by tsunami, sandwiched between peats at Cultus Bay, Washington State. The markings on the shovel are at 0.1 m intervals. The tsunami event was radiocarbon-dated from *Triglochin* rhizomes in the upper peat at AD 1040–1150. Photograph courtesy of Prof. John Clague, Simon Fraser University.

and deposited on the beach. Smaller benthonic and the suspended planktonic species are moved offshore in backwash or transported alongshore in currents to quiescent locations such as estuaries or the low-energy end of a beach. Storm wave conditions tend to move sediment, including diatoms and foraminifera, offshore in backwash, undertow, or rips. However, winds can blow surface waters to shore. A storm assemblage includes very small diatoms or foraminifera diluted with larger, benthonic foraminifera reworked from pre-storm beach sediments. Tsunami assemblages are chaotic because a tsunami wave moves water from a number of distinctive habitats that include marine planktonic and benthic, intertidal, and terrestrial environments. A high proportion of the forams and diatoms are broken, with spherical-shaped species being overrepresented because of their greater resistance to erosion. Storm waves are incapable of flinging debris beyond cliff tops, whereas tsunami can override headlands more than 30 m high. In the latter case, the occurrence of coarse, inshore benthonic species in the debris indicates a marine provenance for the sediment. Where this material is mixed with gravels or other coarse material, it forms one of the strongest depositional signatures of tsunami.

Foram and diatom assemblages have been studied for a number of historic and paleo-tsunami events. For example, the 1 m thick sand layers deposited by the Flores tsunami of December 12, 1992 contain planktonic species such as *Coscinodiscus* and

Cocconeis scutellum as well as the freshwater species *Pinnularia*. The Burin Peninsula tsunami of November 18, 1929 deposited a distinct diatom signature throughout the 25 cm thick sand units in peat swamps. While the peats contain only freshwater assemblages, the tsunami sands contain benthic and intertidal mudflat species such as *Paralia sulcata* and *Cocconeis scutellum*. Freshwater species are incorporated in the lowermost part of the sands, indicating that material was ripped up from the surface of the bogs as the tsunami wave swept over them. Finally, tsunami deposits in eastern Scotland attributable to the Storegga slide 7,950 years ago contain *Paralia sulcata*, which is ubiquitous in the silty, tidal flat habitats of eastern Scotland. The freshwater species *Pinnularia* is also present, indicating that bog deposits were eroded in many locations by the passage of the tsunami wave.

Boulder floaters in sand

(Bryant, Young, and Price, 1992, 1996)

Boulders are not usually transported along sand beaches under normal wave conditions. Their presence as isolated floaters within a sand matrix is therefore suggestive of rapid, isolated transport under high-energy conditions. In many cases, deposits containing boulders are less than 1.5 m thick and lie raised above present sea level along coastlines with stable sea level histories. Either storm waves superimposed

Figure 3.6. Photograph of the coastal landscape at Riang–Kroko on the island of Flores, Indonesia, following the tsunami of December 12, 1992. The greatest run-up height of 26.2 m above sea level was recorded here. Boulders and gravels have been mixed chaotically into the sand sheet. Note the isolated transport of individual boulders. Photo credit: Harry Yeh, University of Washington. *Source:* National Geophysical Data Center.

upon a storm surge or tsunami are known to be responsible for such deposits. For example, Hurricane Iniki in Hawaii in 1992 swept a thin carpet of sand containing boulders inland beyond beaches, while the tsunami that hit Flores, Indonesia, on December 12, 1992 did likewise (Figure 3.6). While storms can exhume boulders lying at the base of a beach and are known to move boulders alongshore, they cannot deposit sand and boulders together on a beach unless overwash is involved.

The cause of boulder floaters in paleo-deposits is difficult to determine unless such deposits lie above the limits of storms. For example, 0.2 m–0.4 m boulder floaters are common within sand deposits south of Sydney along the east coast of Australia (Figure 3.3a). The coastline is tectonically stable, and sea levels have not been more than 1 m higher than present. Here, many deposits lie perched on slopes to elevations of 20 m above sea level, well above the maximum limit of storm surges. Bouldery sands also appear behind beaches where the nearest source for boulders lies up to a kilometer away. Unfortunately, boulder floaters as a signature of tsunami are not an easily recognized one in the field. Boulder floaters often constitute less than 0.1% by volume of a deposit and lie buried beneath the surface. These facts make them difficult to find unless the deposits are trenched or intensively cored.

Dump deposits

(Bryant, Young, and Price, 1992, 1996; Branney and Zalasiewicz, 1999; Kelletat and Schellmann, 2002; Scheffers and Kelletat, 2003, 2005; Kelletat and Scheffers, 2004; Scheffers, 2004)

Chaotic sediment mixtures, or dump deposits, are emplaced in coherent piles or layers above the limits of storm waves, mainly on rocky coasts. They can be problematic. Such deposits can also be formed by solifluction, ice push, slope wash, glowing volcanic avalanches, and human disturbance. Dump deposits were first identified along the south coast of New South Wales, Australia (Figure 3.3a). Because ice, volcanic activity, and ground freezing are not present along this coast, catastrophic tsunami became a viable mechanism for the transportation and deposition of large volumes of sediment with minimal sorting in a very short period. Coarser dump deposits, containing an added component of cobble and boulders, often are plastered against the sides or on the tops of headlands along this coast (Figure 3.7). Many recent deposits may also contain mud lumps. It would be tempting to assign these deposits to storms but for three facts. First, storm waves tend to separate sand and boulder material. Storms comb sand from beaches and transport it into the nearshore zone in backwash and rips. Storm swash, however, moves cobbles and boulders landward and deposits them in storm berms. Certainly, storms do not deposit muds mixed with coarser sediment on steep slopes. On the other hand, tsunami, because of their low height relative to a long wavelength, form constructional waves along most shorelines, transporting all sediment sizes shoreward. Second, while it may be possible for exceptional storms to toss sediment of varying sizes onto cliff tops more than 15 m above sea level, tsunami dump deposits can be found not only much higher above sea level (Figure 3.7), but also in sheltered positions. Finally, there is sub-

Figure 3.7. A chaotically sorted dump deposit on Minnamurra Headland, New South Wales, Australia. The deposit, set in a mud matrix, lies on basalt, yet contains rounded metamorphic beach-worn pebbles. Similar deposits on adjacent headlands contain shell bits. The site is 40 m above sea level on a coast where sea level has been no more than 12 m higher than the present over the past 7,000 years.

stantial observation from Hawaii and elsewhere of tsunami laying down dump deposits (Figure 3.6).

The internal characteristics, or fabric, of tsunami dump deposits allude hydrodynamically to their mode of transport and deposition. This fabric is identical to that formed by pyroclastic density currents or ash clouds emanating from volcanic eruptions. In a pyroclastic flow, fine particles are suspended and transported by turbulent whirlwinds of gas. While appearing as choking clouds of ash, the particles are so widely spaced that they rarely collide. As these turbulent eddies pass over a spot, they can deposit alternating layers of coarse and fine sediment as the velocity of the current waxes and wanes in a similar fashion to gusts of wind. Where the cloud meets the ground, conditions are different. Sediment concentrations increase and sediment particles ranging in size from silts to boulders undergo billions of collisions. The momentum of the flow is equalized between the particles and the flowing current of air. In some cases, the grains may flow independent of any fluid, a phenomenon known as granular flow. Granular flow tends to expel coarse particles to the surface; however, if fluid moves upward through the flow, then a process called fluidization may allow sediment particles in dense slurries to move as a fluid and remain unsorted. Different processes probably operate at different levels in pyroclastic flows. Turbulence lifts finer particles into the current higher up, while at ground level it enhances fluidization. Similarly, the falling out of particles from slurries near the ground

entraps smaller particles into a deposit while expelling water. The latter process also enhances fluidization. From time to time, turbulent vortices penetrate to the bed, allowing the deposition of alternating layers of fine and coarse material. The resulting product is a disorganized deposit containing a wide range of particle sizes with evidence of layering.

All of these characteristics appear in tsunami dump deposits with water taking the place of gas. Alternating layers of fine and coarse sands can be found as small, eroded blocks embedded in chaotically sorted piles of bouldery sand. The layers were deposited from downward turbulent pulses of water that penetrated to the bed. Chipped gravels and shells form deposits that can also contain fragments that show no evidence of violent transport. The former are milled by the myriad of collisions occurring in granular flow toward the base of the current, while the latter have settled from the less dense upper regions of flow. Preservation of fragile particles indicates that deposition must have been rapid. Mud clasts are evidence of the erosive power of turbulent vortices impinging upon the bed. Some of the mud clasts are caught in the granular flow and are disaggregated to form the mud matrix. Some clasts are suspended higher into the less dense part of the flow and are later mixed into the deposit unscathed. Not only do turbulent vortices create spatial variation in the internal fabric of the deposits, they also account for the rapid spatial variation in the degree of erosion of the landscape upstream. Hence, the eroded upstream sides of headlands that provide the material incorporated into dump deposits can still evince weathered soil profiles within meters of bedrock surfaces that have undergone the most intense erosion by vortices.

The rocky headlands of the New South Wales coast also show an unusual variation of dump deposits with a strong Aboriginal constituent. At 16 locations, Aboriginal kitchen middens have been reworked by tsunami. Kitchen middens are trash heaps containing discontinuous layers of edible shell species mixed with charcoal, bone fragments, and artifact stone chips, set in humic-rich sands. All of the disturbed sites incorporate, as an added component, marine shell grit, water-worn shells, rounded pebbles, or pumice. Humus is usually missing from the reworked deposits. Chronology, based upon the suite of signatures present along this coast, suggests that the deposits are only 500 years old. In many cases, the reworked deposits are overlain by undisturbed midden devoid of pumice. Storm waves can be ruled out because many of the sites are situated in sheltered locations or at excessive heights. Storm waves also tend to erode shell and sand-sized sediment seaward and do not deposit bodies of mixed debris several meters thick at the point of run-up on steep backshores at these high elevations. The fact that many of these disturbed middens still contain a high proportion of midden material indicates that disturbance was rapid and incomplete with an input of contaminants from a nearby marine source. Other signatures of tsunami surround all sites. The importance of these disturbed middens will be discussed later in Chapter 8.

Dump deposits have also been described elsewhere—for example, at Stavros, Greece; the south coast of Spain; Cyprus; the Caribbean; the Bahamas; and the southern Ryukyu Islands of Japan. At Stavros, the gravel deposits cover several areas ranging in size between 2.5 m^2 and 250 m^2, deposited up to 40 m from shore.

Some of these deposits are located on cliff tops 10 m above sea level or contain marine molluscs such as *Barbatia barbatia*, *Chamelea striatula*, *Mitra cornicula*, and *Monodonta turbinata*. The Spanish deposits consist of shell fragments, rounded but broken pebbles and cobbles, and rounded boulders up to several 100 kg in weight. The deposits appear to be related to the November 1, 1755 Lisbon tsunami. Those in Cyprus are similar. Mixtures of sand, shell, rounded cobbles, and boulders can be found up to 15 m above sea level. In the Caribbean, dump deposits have been identified on the islands of Guadeloupe, St. Lucia, Grenada, Aruba, Curaçao, and Bonaire. On Guadeloupe and St. Lucia, such deposits reach up to 50 m above sea level and contain boulders up to 10 tonnes in weight. On these islands and the Bahamas, the tsunami events responsible for the dump deposits may be as young as 300–400 years. Often these dump deposits, especially in the Caribbean region, are eroded by heavy rainfalls that have removed sand and silt, leaving behind a lag of exhumed boulders. So pervasive are dump deposits that they can be considered a universal signature of tsunami that have overwashed rocky environments such as cliffs, coastal platforms, and coral reefs where there is a variety of sediment sizes available for transport.

Mounds and ridges

(Minoura and Nakaya 1991; Bryant, Young, and Price, 1992; Bryant *et al*., 1997)

Chaotic dump deposits can be molded into isolated ridges and mounds. These deposits often rise to heights of 3 m or more above the limits of modern storm wave activity. None of these deposits can be explained satisfactorily by ordinary wave processes. For example, at Bass Point 80 km south of Sydney, Australia, a ridge has been sculptured into mounds standing 2 m–3 m in elevation. The mounds consist of chaotically sorted shell hash mixed with rounded cobble and boulder-sized debris. The mounds extend 100 m alongshore and lie 5 m–10 m seaward of a scarp cut into sand dunes. As the shoreline becomes more sheltered, the mounds merge into a 10 m to 20 m wide bench consisting of the same material and rising steeply to a height of 4 m–5 m above the present storm wave limit. The mounds are not unlike the shell mounds formed by tsunami in Japan; however, they are an order of magnitude larger. Slopes on both sides of the mounds exceed 20°, a value that is much steeper than the 7°–9° found on equilibrium profiles formed by storm waves in similarly sized material. A chaotic sheet of cobble and boulder material protruding through a shell hash matrix fronts the mounds. This sheet rests on a seaward-sloping bedrock platform. The fact that this debris is partially vegetated suggests that present storm wave run-up has not affected it. The mounds were deposited within vortices created in the lee of a 15 m high headland that was overwashed by a large tsunami.

There are several examples of ridges formed by tsunami. On the island of Lanai in Hawaii, boulder deposits supposedly deposited by tsunami evince ripple forms 1 m high with a spacing of 100 m between crests. On the South Ryukyu Islands in Japan, ridges several meters high and 40 m wide have been linked to tsunami. However, among the most unusual coastal features are the chenier-like ridges formed in Batemans Bay on the New South Wales coast of Australia (Figure 3.3a). Cheniers

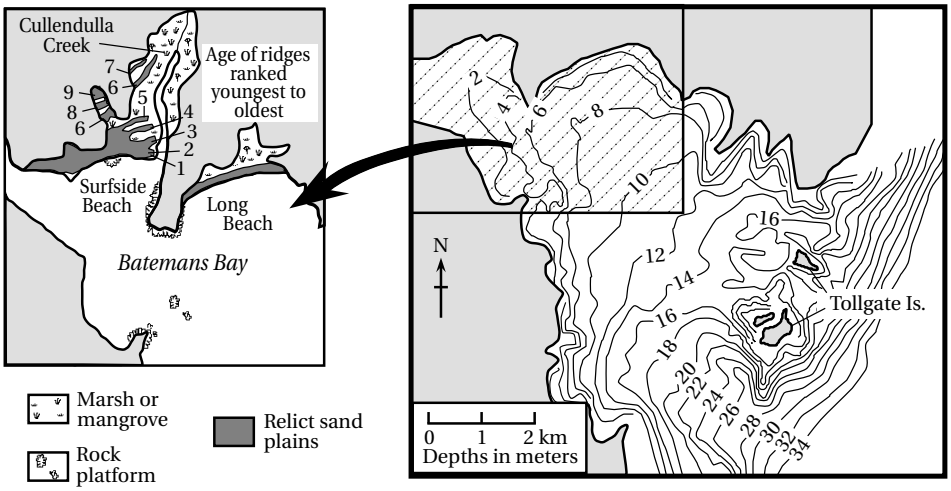

Figure 3.8. The chenier-like ridges in the Cullendulla Creek embayment at Batemans Bay, New South Wales, Australia. From Bryant, Young, and Price (1992).

are ridges of coarser sediment usually deposited at the limit of storm waves in muddy environments. Batemans Bay is a 14.4 km long, funnel-shaped, sand-dominated embayment that averages 11 m in depth and semi-compartmentalized by north–south structurally controlled headlands (Figure 3.8). This shape is conducive to resonance and enhancement of tsunami entering from the open ocean. The basin's resonance periods are 4.5 min, 13.4 min, 22.5 min, and 31.0 min, values that fall within the range of typical tsunami periods measured in harbors. The cheniers in the bay consist of a series of six ridges deposited in a sheltered embayment presently occupied by Cullendulla Creek (Figure 3.8). The ridges rise 1.0 m–1.5 m above the surrounding estuarine flats and increase in width and volume toward the bay, where they merge into a barrier complex consisting of at least eight ridges. The cheniers consist of shell-rich sand overlying estuarine muds. They are asymmetric in shape, rising steeply to a height of 0.5 m–0.6 m and then dropping landward over a 30 m to 40 m distance to the estuarine surface. The ridges also extend as raised banks 1 km up a creek entering on the western side of the embayment. The banks are 30 m–40 m wide and stand 0.75 m–1.0 m above the high-tide limit. The innermost bank contains shell species derived from sheltered rocky shores, open ocean beaches, rock platforms, and the inner continental shelf.

The formation of these chenier ridges by storm waves is difficult to justify because wave refraction reduces wave heights by 80% to 90%. Waves would have to travel in the most convoluted pathway possible to deposit ridges up the re-entrant within Cullendulla Creek. This includes passing through a gap 600 m wide at the most sheltered part of the embayment, bending 500 m behind a large rock promontory, and traveling up the shallowing re-entrant for a distance of 600 m. The simpler explanation is that tsunami have deposited chenier-like ridges and banks in this

sheltered re-entrant. There is chronological evidence for at least three tsunami events operating within the bay 300 yr, 1,300 yr, and 2,800 yr ago. While Batemans Bay contains the best example of tsunami ridge development along this coast, similar ridges and banks exist in the Port Hacking, Middle Harbor, and Patonga Beach estuaries in the Sydney area 200 km to the north. Spits and ridges lying within sheltered estuarine environments should be examined closely for evidence of a tsunami origin.

Chevrons and dune bedforms

(Ota *et al.*, 1985; Bryant *et al.*, 1997; Hearty, Neumann, and Kaufman, 1998; Kelletat and Scheffers, 2003)

Tsunami can also create dunes. These take two forms: those that back beaches and can easily be misinterpreted as parabolic, wind-blown sand dunes, and those that form as bedforms under catastrophic unidirectional flow generated by large tsunami. The former are sandy, but contain angular clasts or mud layers that cannot be transported or deposited by wind. These types of ridges exist on Hateruma Island in the South Ryukyus of Japan, where they consist of sand, gravels, and large boulders up to 2 m in width. They were deposited by the great tsunami of April 24, 1771, which had a maximum run-up height in the region of 85.4 m. Another example occurs at the south end of Jervis Bay, New South Wales (Figure 3.3a). Here a parabolic dune, rising more than 130 m above sea level, contains gravels and mud clasts (Figure 3.9). Because these tsunami swash features are symmetrical, they form V-shaped dunes that may be stacked relative to each other. They are also called chevrons after the inverted "V" used in heraldry or the stripes on the arms of a military uniform used to denote rank. This term comes from similarly shaped dunes found in Barbados and dating to the Last Interglacial.

The chevron feature in Jervis Bay is contiguous in form, from the present beach to a peak 130 m above present sea level. It is an exemplary signature of mega-tsunami because its limits are far beyond those of either storm swash or earthquake-generated tsunami reported in the literature. Four waves are envisaged to have formed the feature (Figure 3.10). The first wave was depositional, overwashing the hill 130 m above sea level and depositing most of the sediment in the chevron. The second wave was probably larger; but because most of the available sediment had already been moved onshore, it eroded the seaward portion of the chevron deposited by wave 1. It overwashed the previous deposit and moved a small amount of sediment farther inland at the crest. Backwash seaward down the chevron was minimal for each of these waves, because most of the water flowed over the hill. The third wave was smaller and did not reach the crest of the chevron. It didn't bring any sediment to the coast and backwash under the effect of gravity eroded into the central trough of the chevron. The final wave was smaller still and its backwash enhanced erosion in the trough. The resulting form of the chevron is thus depositional at its landward end and sides, but erosional at its seaward end and along the central axis. The sediments shown in Figure 3.9 are located halfway up the flank of the chevron at location C.

Figure 3.9. Fabric of sand and gravel deposited in a chevron-shaped dune by paleo-tsunami at Steamers Beach, Jervis Bay, Australia. Car keys are for scale. The rounded ball to the left of the keys consists of humate eroded elsewhere from the B-horizon of a podsolic soil profile. This deposit lies 30 m above sea level, while the dune itself crests 130 m above sea level.

Independently, Kelletat and Scheffers (2003) examined the orientation of parabolic dunes around Australia. They found that their orientation did not match prevailing winds and could not be wind-formed. If correct, and their hypothesis is extended to other coasts, then chevrons represent the signature of mega-tsunami worldwide. Only large submarine landslides or comet/asteroid impacts with the ocean can account for these common, large-scale features.

Dune bedforms are created under catastrophic flow. Such features were first described in the scablands of Washington State. The scablands consist of a series of enormous dry canyons occupied by gigantic rippled sandbars. The catastrophic flow originated from the collapse of an ice dam holding back glacial Lake Missoula in the Northern Great Plains of the United States during the last Ice Age. Repetitive floods up to 30 m deep spread across sandy plains, creating enormous dune bedforms. Similar dune bedforms can be produced by large tsunami. Two examples have been identified. The first is located at Crocodile Head, north of the entrance to Jervis Bay, Australia. Here, sandy ridges containing pebbles and gravels appear as a series of well-defined, undulatory-to-linguoidal giant ripples spread over a distance of at least 1.5 km atop 80 m high cliffs. These mega-ripples have a relief of 6.0 m–7.5 m, are

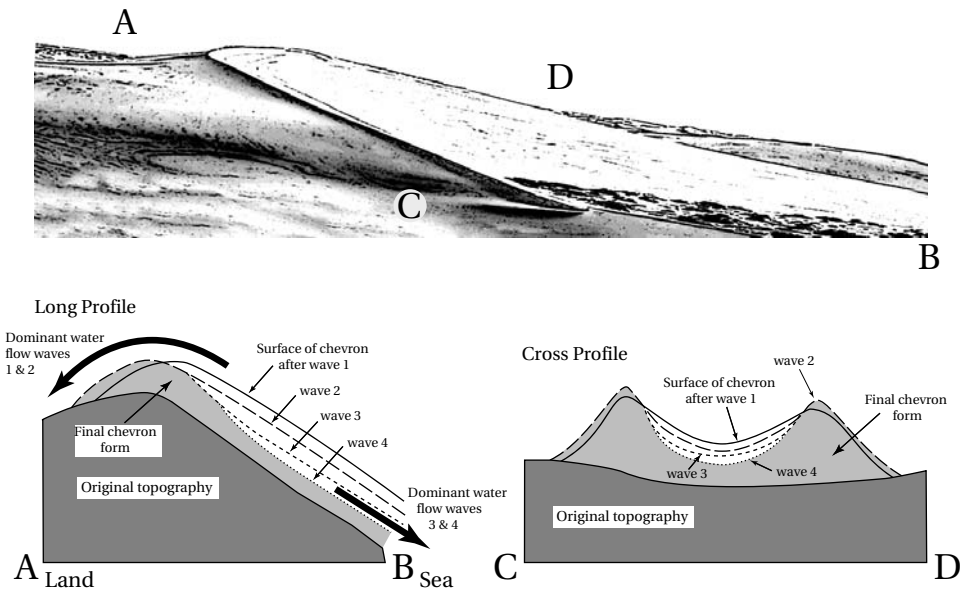

Figure 3.10. Schematic representation of the formation of a chevron dune at Steamers Beach, Jervis Bay, New South Wales, Australia due to tsunami.

asymmetric in shape, and spaced 160 m apart. The mega-ripple field is restricted to a 0.5 m to 0.7 km wide zone along the cliffs, and is bounded landward by a linear ridge of sand several meters high paralleling the coastline. This ridge is flanked by small depressions. Farther inland, deposits grade rapidly into hummocky topography, and then a 1 m to 2 m thick sandsheet. The mega-ripples were produced by sediment-laden tsunami overwashing the cliffs, with subsequent deposition of sediment into bedforms along the cliff top. Flow then formed an overwash splay as water drained downslope. The flow over the dunes is theorized to have been 7.5 m–12.0 m deep and to have obtained velocities of 6.9 m s^{-1}–8.1 m s^{-1}. The second example occurs at Point Samson, Western Australia (Figure 3.3c). Here gravelly mega-ripples have infilled a valley with bedforms that have a wavelength approaching 1,000 m and an amplitude of about 5 m. Flow depth is theorized to have been as great as 20 m with velocities of over 13 m s^{-1}.

Smear deposits

More enigmatic are deposits on headlands containing a mud matrix. These deposits are labeled smear deposits because they are often spread in a continuous layer less than 30 cm thick over the steep sides and flatter tops of headlands. Along the New South Wales coast, these deposits have been found at elevations 40 m above sea level. These deposits can contain 5% to 20% quartz sand, shell, and gravel. Smear deposits

are not the products of *in situ* weathering because many can be found on volcanic sandstone or basalt, which lacks quartz. These smear deposits form the traction carpet at the base of a sediment-rich tsunami-generated flow overwashing headlands. The mud allows sediment to be spread smoothly under substantial pressure over surfaces. When subsequently dried, the packed clay minimizes erosion of the deposit by slope wash on steep faces. The deposit has only been identified on rocky coasts where muddy sediment lies on the seabed close to shore.

Large boulders and piles of imbricated boulders

(Baker, 1978; Moore and Moore, 1988; Kawana and Pirazzoli, 1990; Kawana and Nakata, 1994; Young, Bryant, and Price, 1996; Bryant *et al.*, 1997; Nott, 1997; Kelletat and Schellmann, 2002; Cass and Cass, 2003; Nott, 2003; Scheffers, 2004)

Tsunami differ from storm waves in that tsunami dissipate their power at shore rather than within any surf zone. The clearest evidence of this is the movement of colossal boulders onshore. For example, the Flores tsunami of December 12, 1992 destroyed sections of fringing reef and moved large coral boulders shoreward (Figure 3.6), often beyond the zone where trees were ripped up by the force of the waves. The Sea of Japan tsunami of May 26, 1983 produced a tsunami over 14 m high. A large block of concrete weighing over 1,000 tonnes was moved 150 m from the beach over dunes 7 m high. Boulders transported by tsunami have also been found in paleo-settings. For example, on the reefs of Rangiroa, Tuamoto Archipelago in the southeast Pacific, individual coral blocks measuring up to 750 m^3 have been linked to tsunami rather than to storms. Boulders have also been scattered by tsunami across the reefs at Agari-Hen'na Cape on the eastern side of Miyako Island in the South Ryukyu Islands (Figure 3.11). On Hateruma and Ishigaki Islands in the same group, coralline blocks measuring 100 m^3 in volume have been emplaced up to 30 m above present sea level, 2.5 km from the nearest beach. These boulders have been dated and indicate that tsunami, with a local source, have washed over the islands seven times in the last 4,500 years. Two of the largest events occurred 2,000 years ago and during the great tsunami of April 24, 1771. In the Leeward Islands of Netherlands Antilles in the Caribbean, boulders weighing up to 280 tonnes have been moved 100 m by repetitive tsunami most likely occurring 500, 1,500, and 3,500 years ago. In fact, detailed cataloging of anomalous boulders from the literature indicates that they are a prevalent signature of tsunami on most coasts. The largest boulder theorized as being transported by tsunami occurs at Port Stephens in the Bahamas. It weighed 2,000 tonnes and was moved 500 m inland to an elevation of 11 m above sea level.

Along the east coast of Australia, anomalous boulders are incompatible with the storm wave regime. For example, exposed coastal rock platforms along this coast display little movement of boulders up to 1 m–2 m in diameter, despite the presence of 7 m to 10 m high storm waves. At Boat Harbor, Port Stephens (Figure 3.3a), blocks measuring 4 m × 3 m × 3 m not only have been moved shoreward more than 100 m, but also have been lifted 10 m to 12 m above existing sea level. At Jervis Bay, preparation zones for block entrainment can be found along cliff tops 15 m above sea

Figure 3.11. Scattered boulders transported by tsunami and deposited across the reef at Agari-Hen'na Cape on the eastern side of Miyako Island, Ryukyu Island, Japan. Photograph courtesy of Prof. Toshio Kawana, Laboratory of Geography, College of Education, University of the Ryukyus, Nishihara, Okinawa.

level. Contentious is the documented appearance of a 200-tonne boulder measuring 6.1 m × 4.9 m × 3.0 m on an intertidal rock platform during a storm in 1912 at Bondi Beach, Sydney. However, Cass and Cass (2003) show that the boulder appears in an 1881 photograph. It has not moved since, even during the great storms of 1876, 1889, 1912, and 1974—the latter judged the worst in a hundred years. While much higher storm events can be, and have been, invoked for the movement of the boulders now piled prodigiously along this coast, tsunami offer a simpler mechanism for the entrainment of joint-controlled blocks, the sweeping of these blocks across platforms, and their deposition into imbricated piles.

In exceptional cases, boulders have been deposited as a single-grained swash line at the upper limit of tsunami run-up. Some of these tsunami swash lines lie up to 20 m above sea level and involved tractive forces greater than 100 kg m^{-2}. Just as unusual are angular boulders jammed into crevices at the back of platforms. For instance, at Haycock Point, north of the Victorian border, angular blocks up to 2 m in length and 0.5 m in width have been jammed tightly into a crevice, often in an interlocking series three or four blocks deep. What is more unusual about the deposit is the presence along the adjacent cliff face of isolated blocks 0.4 m–0.5 m in length perched in crevices 4 m–5 m up the cliff face. Boulders are also found in completely sheltered locations along the coast. At Bass Point, which extends 2 km seaward from the coast, a boulder beach faces the mainland coast rather than the open sea. Similarly at Haycock Point, rounded boulders, some with volumes of 30 m^3 and weighing

Figure 3.12. Boulders transported by tsunami down a ramp in the lee of the headland at Haycock Point, New South Wales, Australia. This corner of the headland is protected from storm waves. The ramp descends from a height of 7 m above sea level. Its smooth undular nature is a product of bedrock sculpturing.

75 tonnes, have been piled into a jumbled mass at the base of a ramp that begins 7 m above a vertical rock face on the sheltered side of the headland (Figure 3.12). Chatter marks on the ramp surface indicate that many of the boulders have been bounced down the inclined surface.

Perhaps the most dramatic deposits are those containing piles of imbricated boulders. These piles take many forms, but include boulders up to 106 m^3 in volume and weighing as much as 286 tonnes. The boulders lie *en echelon* one against the other like fallen dominoes, often in parallel lines. At Jervis Bay, New South Wales, blocks weighing almost 100 tonnes have clearly been moved in suspension and deposited in this fashion above the limits of storm waves on top of cliffs 33 m above present sea level (Figure 3.13). The longest train of imbricated boulders exists at Tuross Head where 2 m to 3 m diameter boulders stand as sentinels one against the other, over a distance of 200 m at an angle to the coast.

The velocity of water necessary to move these large boulders can be related to their widths as follows:

$$\bar{v} = 5.2B_I^{0.487} \tag{3.1}$$

$$v_{\min} = 2.06b^{0.5} \tag{3.2}$$

where $\bar{v}$ = mean flow velocity ($m\,s^{-1}$)
$v_{\min}$ = minimum flow velocity ($m\,s^{-1}$)

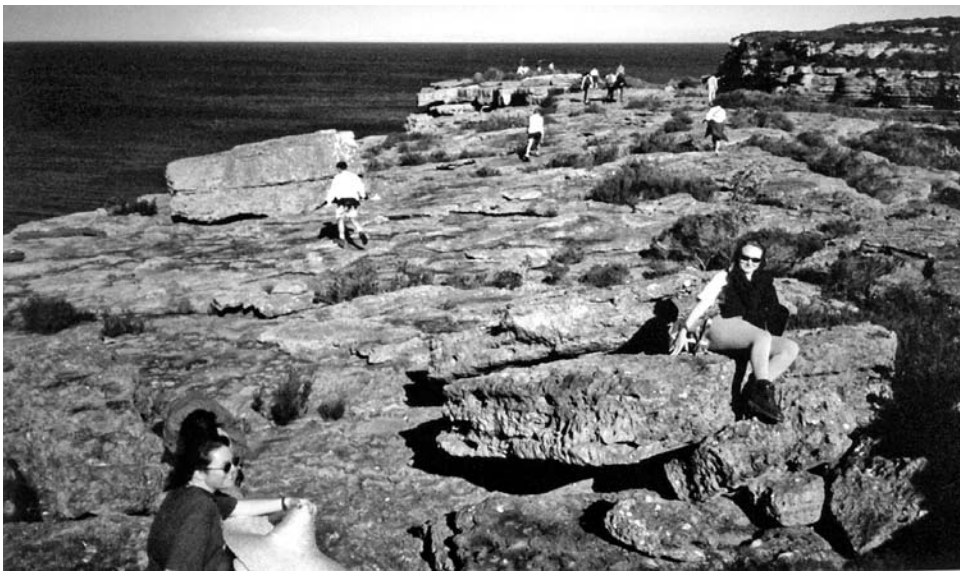

Figure 3.13. Dumped and imbricated sandstone boulders deposited 33 m above sea level along the cliffs at Mermaids Inlet, Jervis Bay, Australia. Note the eroded surface across which waves flowed from left to right.

b = the intermediate axis or width of a boulder (m)
b_I = intermediate diameter of largest boulders (m)

Table 3.2 presents the theorized velocities of tsunami flow required to move the boulders found along the New South Wales coast using these two equations. The minimum theoretical flow velocity ranges between $2.2\,\mathrm{m\,s^{-1}}$–$4.2\,\mathrm{m\,s^{-1}}$. Mean flows appear to have exceeded $5\,\mathrm{m\,s^{-1}}$ with values of $7.8\,\mathrm{m\,s^{-1}}$–$10.3\,\mathrm{m\,s^{-1}}$ being obtained on exposed ramps or at the top of cliffs.

It is more useful to be able to determine flow depth because, as shown in the previous chapter, this equates to the height of the tsunami wave at shore—Equation (2.15). Boulders occupy three different environments in the coastal zone. They can exist exposed singly along the coast on dry land such as on a rock platform (term sub-aerial), be submerged, or be part of a bedrock surface. In the latter case, boulders have to be ripped from this surface, usually along joints, before they can be transported. The boulders are thus joint bound. Boulder transport will be initiated for each of these situations by a tsunami wave, whose height at the shoreline is H_t, when the following relationships are met:

$$\text{Sub-aerial:} \quad H_t \geq 0.5a\{[(\rho_s - \rho_w)\rho_w^{-1}] - [\ddot{u}aC_m(bg)^{-1})]\}[C_d(acb^{-2}) + C_l]^{-1} \tag{3.3}$$

$$\text{Submerged:} \quad H_t \geq 0.5a[(\rho_s - \rho_w)\rho_w^{-1}][C_d(acb^{-2}) + C_l]^{-1} \tag{3.4}$$

$$\text{Joint bound:} \quad H_t \geq 0.25a[(\rho_s - \rho_w)\rho_w^{-1}]C_l^{-1} \tag{3.5}$$

Table 3.2. Velocities and wave heights of tsunami as determined from boulders found on headlands along the New South Wales coast.

Location	*Size* (m)	*Mean velocity* ($m\,s^{-1}$)	*Lowest velocity* ($m\,s^{-1}$)	*Wave height* (m)
Jervis Bay				
Mermaids Inlet	2.3	7.8	3.1	1.4
Little Beecroft Head				
Ramp	4.1	10.3	4.2	2.7
Clifftop	1.2	5.6	2.2	0.7
Honeysuckle Point	2.8	8.6	3.4	1.8
Tuross Head	1.3	5.9	2.3	0.8
Bingie Bingie Point	2.8	8.6	3.4	1.8
O'Hara Headland	1.1	5.5	2.2	0.7

Note: Sediment size refers to the mean width of the five largest boulders.
Source: Based on Young, Bryant, and Price (1996).

where H_t = wave height at shore or the toe of a beach
a = boulder length (m)
c = boulder thickness (m)
ρ_s = density of a boulder (usually $2.7\,g\,cm^{-3}$)
ρ_w = density of sea water (usually $1.024\,g\,cm^{-3}$)
C_d = the coefficient of drag (typically 1.2 on dry land)
C_l = the coefficient of lift, typically 0.178
C_m = the coefficient of mass, typically 2.0
$\ddot{u}$ = instantaneous flow velocity ($m\,s^{-1}$), typically $1\,m\,s^{-1}$

Note that the tsunami heights estimated by these equations are conservative because the equation uses the velocity of a tsunami wave in shallow water—Equation (2.2)—rather than the higher velocity that is possible across dry land—Equation (2.16). Equation (3.4) for submerged boulders is the commonest situation and is used throughout this book. This equation can be simplified by substituting in the parameters listed after Equation (3.5). It can be further simplified if the boulders being transported are nearly spherical. These simplifications are expressed as follows:

$$\text{Simplified:} \quad H_t \geq 0.82a(1.2acb^{-2} + 0.178)^{-1} \tag{3.6}$$

$$\text{For spheres:} \quad H_t \geq 0.6b \tag{3.7}$$

The crucial parameter in the movement of boulders is the drag force, and this is very sensitive to the thickness of the boulder. The thinner the boulder, the greater the velocity of flow required to initiate movement. Thickness is even more important than mass or weight. This point is illustrated in Figure 3.14 for two boulders of equal length and width but different thicknesses. Despite being four times larger in volume

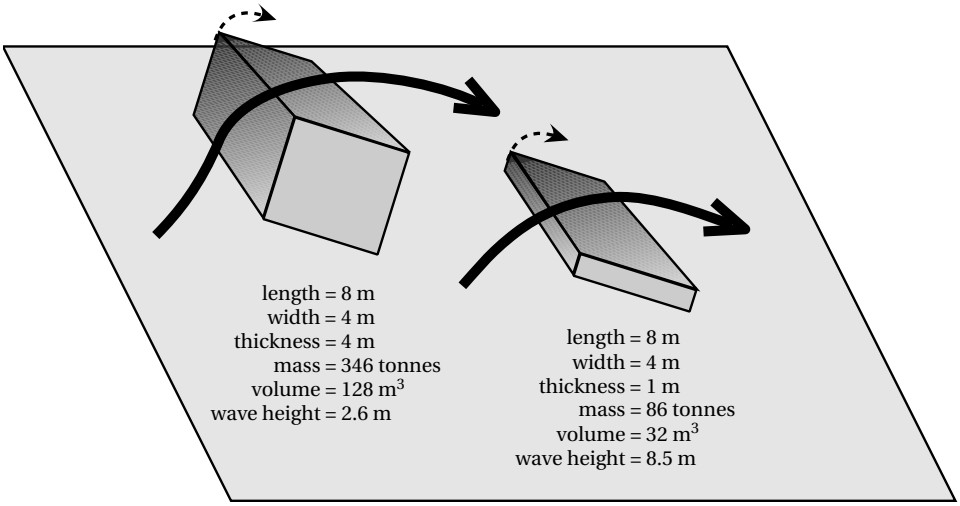

Figure 3.14. Illustration of the forces necessary to entrain two boulders having the same length and width, but different thicknesses.

and weight, the rectangular boulder only requires a tsunami wave that is one-third of the height of the wave needed to move the platy one. This effect is also illustrated in Figure 3.12. All of the boulders shown on the ramp required the same depth of water to be moved, despite the spherical ones being twice as large as the flatter ones.

Equation (3.12) has practical application for determining the height of a tsunami wave based upon the size of debris found afterwards. For instance, the largest boulder transported by the Flores tsunami shown in Figure 3.6 required a tsunami wave of about 2 m in height to move. Note that these flow depths are minimum values, because the tsunami wave would have been much higher at the shoreline than where the boulder was dumped. Calculations of the mean tsunami wave heights required to move boulders in the Jervis Bay region are included in Table 3.2. Boulders in the Jervis Bay region only required a tsunami wave 3 m high to be moved, even though waves higher than this must have been involved in order to transport boulders in suspension up cliffs. These examples illustrate how efficient tsunami waves are at initiating movement of bouldery material. The height of storm waves required to move the same size material is not nearly as small—a point that will be discussed in Chapter 4.

If tsunami wave height at shore equates with flow depth—Equation (2.15)—the height of the tsunami can also be calculated using the spacing between boulder bedforms as follows:

$$H_t = 0.5 L_s \pi^{-1} \tag{3.8}$$

where L_s = bedform wavelength (m)

Figure 3.15. Boulder ripples deposited by tsunami on the rock platform of Jibbon, New South Wales, Australia. The theorized flow with standing waves is shown by the white path. The boulders were deposited under the crest of standing waves generated in the flow, while vortices bored pools into the rock surface in the troughs. Person circled for scale.

However, boulder ripples or dunes are rare in nature. In the Jervis Bay region, boulder piles suggestive of mega-ripples exist at Honeysuckle Point and have a spacing of 60 m. The alignment of individual boulders in one pile, at an elevation of 16 m above sea level, shows the foreset and topset bedding characteristic of a ripple. The minimum tsunami wave height for these features using Equation (3.8) is 9.5 m. This agrees with the flow depth required to construct the giant mega-ripples located nearby at Crocodile Head and described earlier. By far the best site with boulder ripples occurs at Jibbon in the Royal National Park immediately south of metropolitan Sydney. Here at least four ripples are evident over a distance of 100 m (Figure 3.15). Flow swept over the platform at an oblique angle from the south and set up standing waves as velocity was accelerated rising over the platform surface about 2 m–4 m above sea level. Boulders were deposited against each other under the peaks of the standing waves in piles that show clear foreset and topset bedding. In the troughs, where flow impinged upon the rock platform, vortices were generated that carved small pools 40 cm–50 cm in diameter and depth into the bedrock. The latter features are termed bedrock sculpturing and will be described in more detail later.

The following scenario can account for the formation and transport of boulders along rocky coasts. On headlands or rock platforms where there is a cliff or ledge facing the sea, waves have to drown the cliff face before overtopping them. Tsunami do this by jetting across the top of the cliffs and developing a roller vortex in front of the cliff edge. Flow is thus thin (depths of 2.5 m–3.5 m) and violent (minimum velocities typically between $5\,m\,s^{-1}$ and $10\,m\,s^{-1}$). In jets, tsunami flow velocities may exceed $200\,m\,s^{-1}$. High-velocity flow first strips weathered bedrock surfaces of debris, exposing the underlying bedrock to large lift forces. Blocks, controlled in size by the thickness of bedding planes and the spacing of joints, may be too large to be entrained by this tsunami flow, but the lift forces can continually jar blocks until they eventually fracture into smaller pieces. This process occurs in preparation zones at the front of cliffs. When blocks are small enough, they then are transported across headlands or down platform and ramp surfaces. The lack of percussion marks or chipping on most boulders, some of which are highly fretted by chemical weathering,

is suggestive of boulder suspension in sediment-starved flows without bed contact until the boulder is deposited. The minimum flow depth or tsunami wave height along the coast of New South Wales required in this scenario is 4 m, although larger waves must certainly have been present to move such material up cliffs 30 m high (Figure 3.12).

In summary, boulders along coasts most likely relate to tsunami if they meet the following ten criteria: (1) the boulders are in groups; (2) the boulder deposits exclude other sediment sizes; (3) the boulders are imbricated and contact-supported; (4) the points of contact support lack evidence of percussion implicating suspension transport; (5) the boulders show lateral transport or shifting distinctive from *in situ* emplacement due to cliff collapse under gravity; (6) the boulders are elevated above the swash limit for storm waves; (7) the boulders are situated away from any shoreline where storm waves impacting on the coast could have simply flicked material onto shore; (8) the evidence of transport by tsunami rather than storm waves is unequivocal based upon hydrodynamic determinations; (9) the direction of imbrication matches the direction of tsunami approach to the coast regionally; and (10) there are other nearby signatures of tsunami.

Turbidites

(Bouma and Brouwer, 1964; Masson, Kenyon, and Weaver, 1996)

There are few geomorphic features linked to tsunami described in the ocean. However, one of the most notable—turbidites—has received considerable attention in the literature. Submarine landslides generate both tsunami and turbidites. As a submarine landslide moves downslope under the influence of gravity, it disintegrates and mixes with water. The sediment in the flow tends to separate according to size and density, forming a sediment gravity flow called a turbidity current. The slurry in a turbidity current moves along the seabed at velocities between $20\,km\,h^{-1}$ and $75\,km\,h^{-1}$, and can travel thousands of kilometers onto the abyssal plains of the deep ocean on slopes as low as 0.1°. As current velocity decreases, splays of sediment, known as turbidites, are deposited in submarine fans. Turbidite thickness depends upon the distance of travel and the amount of sediment involved in the original submarine landslide. In the Atlantic Ocean, individual turbidites have volumes of $100\,km^3$–$200\,km^3$, values that are sufficient to have generated tsunami of several meters amplitude at their source. Turbidity currents have not been directly observed; however, there is substantial indirect evidence for their existence. One of the best of these is the sequential breaking of telegraph cables laid across the seabed. The first noteworthy record occurred following the Grand Banks earthquake on November 18, 1929 off the coast of Newfoundland. Similar events have occurred off the Magdalena River delta (Colombia), the Congo Delta, in the Mediterranean Sea north of Orléansville and south of the Straits of Messina, and in the Kandavu Passage, Fiji.

Turbidites generally are less than 1 m in thickness and form a distinct layered unit known as a Bouma sequence (Figure 3.16). The upward structure of a Bouma unit shows erosional marks in the underlying clays called sole marks, overlain by a

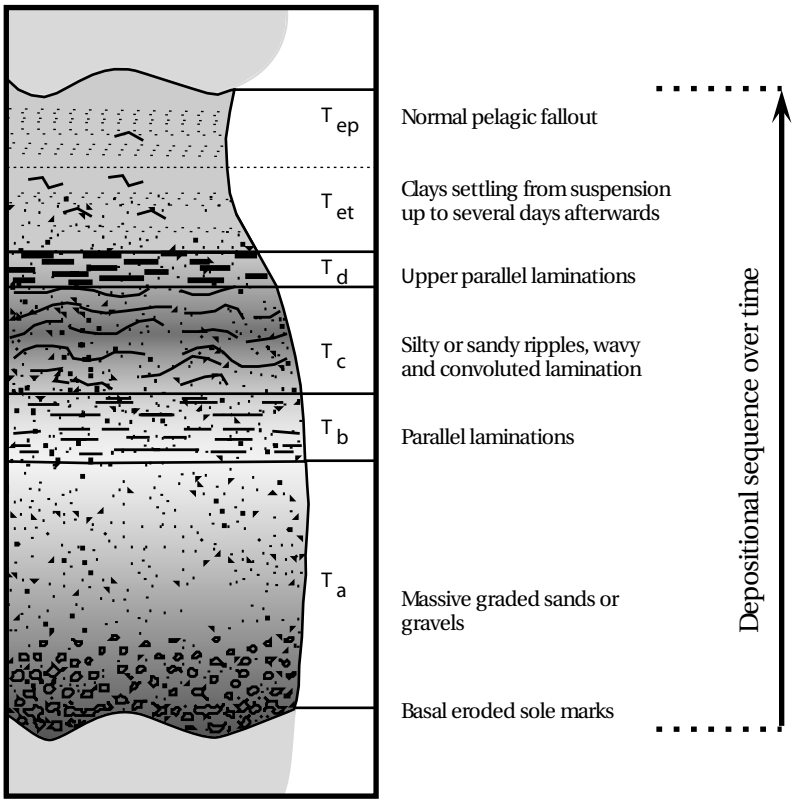

Figure 3.16. A Bouma turbidite sequence deposited on the seabed following the passage of a turbidity current. Based on Bouma and Brouwer (1964).

massive graded unit (T_a), parallel lamination (T_b), rippled cross-lamination or convoluted lamination (T_c), and an upper unit of parallel lamination (T_d). This latter unit contains gravels and pebbles close to the source, and fine sand and coarse silt out on the abyssal plain. The unit is overlain by pelagic ooze (T_{ep}) that has settled under quiet conditions between events. The basal contact below the coarse layer is sharp, while that above is gradational. The coarse layer is also well sorted and contains microfossils characteristic of shallow water. Interpretation of this sequence, supported by laboratory experiments, indicates deposition from a current that initially erodes the seabed, and then deposits coarse sediment that fines as velocity gradually diminishes. More has been written about sediment density flows in sedimentology than on any other topic, and the deposits form one of the most common sedimentary sequences preserved in the geological record. Each turbidity deposit preserved in this record potentially could be a diagnostic signature of a tsunami event. Submarine landslides and their resultant tsunami have been very common features in the world's oceans throughout geological time.

EROSIONAL SIGNATURES OF TSUNAMI

Small-scale features

(Dahl, 1965; Baker, 1981; Kor, Shaw, and Sharpe, 1991; Young and Bryant, 1992; Bryant and Young, 1996; Aalto *et al.*, 1999)

Tsunami can also sculpture bedrock in a fashion analogous to the *S*-forms produced by high-velocity catastrophic floods or surges from beneath icecaps in sub-glacial environments. *S*-forms include features such as muschelbrüche, sichelwannen, V-shaped grooves, cavettos, and flutes (Figures 3.2 and 3.17). They have been linked to paleo-floods in Canada, the northwestern United States, Scandinavia, Britain, the Alps, and the Northern Territory, Australia. Tsunami flow over rocky headlands, at

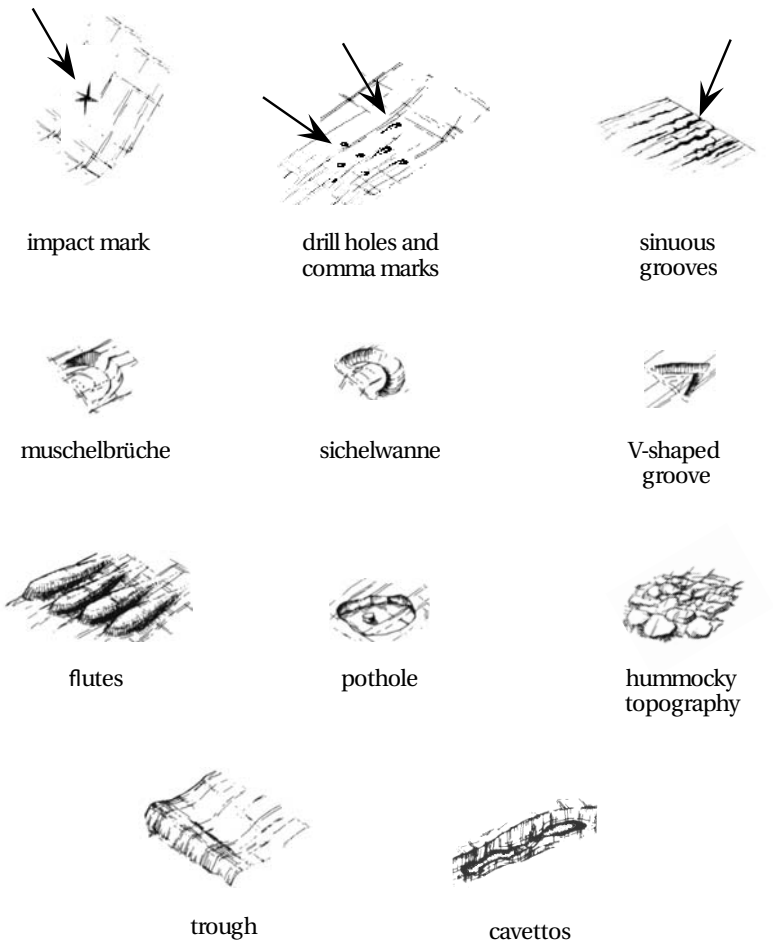

Figure 3.17. Various cavitation features and *S*-forms produced by high-velocity tsunami flow over headlands. Note that the features are not scaled relative to each other.

the velocities outlined in Chapter 2, has the hydrodynamic potential to generate cavitation or small vortices capable of producing sculptured forms. The spatial organization of *S*-forms on headlands, often above the limits of storm waves, is a clear signature of tsunami in the absence of any other definable process. Individual *S*-forms and their hydrodynamics will be described in this chapter, while their spatial organization into unique tsunami-generated landscapes will be discussed in Chapter 4.

Cavitation is a product of high-velocity flow as great as $10\,m\,s^{-1}$ in water depths as shallow as 2 m. At these velocities, small, low-pressure, air bubbles appear in the flow. These bubbles are unstable and immediately collapse, generating impact forces up to 30,000 times greater than normal atmospheric pressure. Cavitation bubble collapse is highly corrasive, and is the reason propeller-driven ships cannot obtain higher speeds and dam spillways have a limited lifetime. In tsunami environments, cavitation produces small indents that develop instantaneously, parallel or at right angles to the flow, on vertical and horizontal bedrock surfaces. Cavitation features are widespread and consist of impact marks, drill holes, and sinuous grooves (Figures 3.2 and 3.17).

Impact marks appear as pits or radiating star-shaped grooves on vertical faces facing the flow. It would be simple to suggest that such features represent the impact mark of a rock hurled at high velocity against a vertical rock face; however, such marks have also been found in sheltered positions or tucked into undercuts where such a process is unlikely (Figure 3.18). Drill holes are found over a range of locations on tsunami-swept headlands. Their distinguishing characteristic is a pit several centimeters in diameter bored into resistant bedrock such as tonalite or gabbroic diorite. Drill holes appear on vertical faces, facing either the flow or at right angles to it. Such marks also appear on the inner walls of large whirlpools. While it would be easy to attribute these features to marine borers, they often occur profusely above the limit of high tide.

The most common type of drill mark appears at the end of a linear or sinuous groove and extends downward at a slight angle for several centimeters into very resistant bedrock. In some cases, grooves also narrow with depth to form knife-like slashes a few centimeters deep. Sinuous drill marks are useful indicators of the direction of tsunami flow across bedrock surfaces. Sinuous grooves tend to extend no more than 2 m in length and have a width of 5 cm–8 cm at most. Depth of cutting can vary from a few millimeters to several centimeters. In some cases, the sinuous grooves become highly fragmented longitudinally and form comma marks similar to those found in sub-glacial environments. Often they form *en echelon* in a chain-like fashion (Figure 3.19). They are not a product of storm waves or backwash because they show internal drainage and do not join downslope. Sinuous grooves have been described for the southeast coast of New South Wales and for platforms near Crescent City, California, where tsunami appear to be a major process in coastal landscape evolution. It is tempting to credit their formation to chemical erosion along joints, micro-fractures, or igneous inclusions. Four facts suggest otherwise. First, while they may parallel joints, sinuous grooves diverge from such structures by up to 10°. Second, joints in bedrock are linear over the distances, which grooves develop.

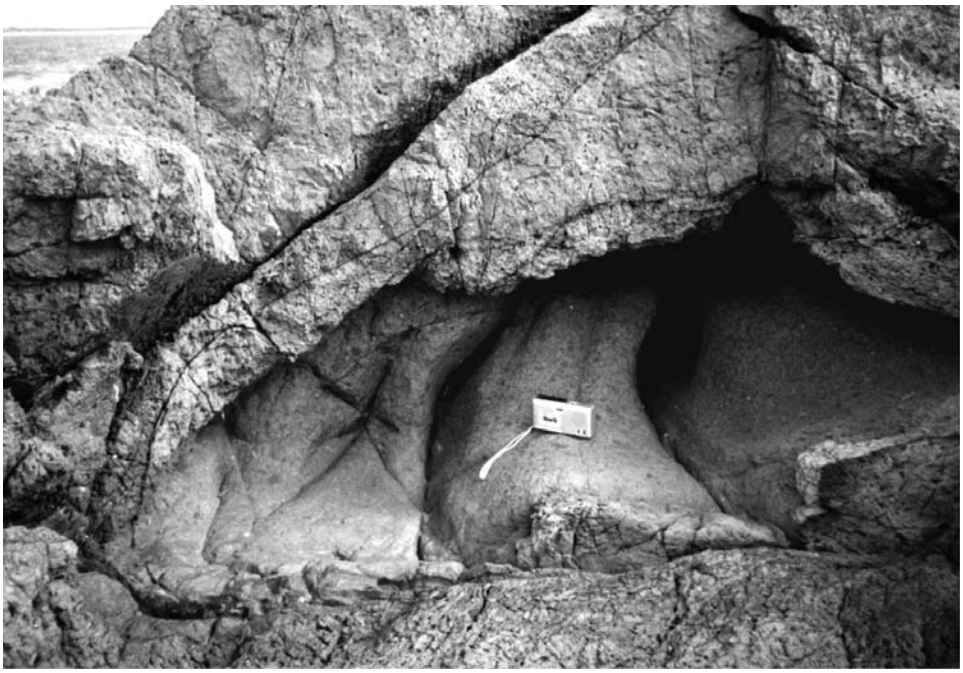

Figure 3.18. A star-shaped impact mark on the face of the raised platform at Bass Point, New South Wales, Australia. Note as well the drill holes. The sheltered juxtaposition of these forms suggests that cavitation rather than the impact of rocks thrown against the rock face eroded them.

The grooves described here are sinuous. Third, sinuous grooves often appear as sets within the spacing of individual joint blocks. Finally, sinuous grooves occur only on polished and rounded surfaces characteristically produced by tsunami, and not on the highly weathered, untouched surfaces nearby.

S-forms also develop on surfaces that are smoothed and polished. This polishing appears to be the product of sediment abrasion. However, high water pressures impinging on bedrock surfaces can also polish rock surfaces. Flow vortices sculpture *S*-forms that can be categorized by the 3-dimensional orientation of these eddies. The initial forms develop under small roller-like vortices parallel to upslope surfaces. In this case muschelbrüche, sichelwanne, and V-shaped grooves are created (Figure 3.17). Muschelbrüche (literally mussel-shaped) are cavities scalloped out of bedrock, often as a myriad of overlapping features suggestive of continual or repetitive formation. While the features appear flat-bottomed, they have a slightly raised pedestal in the center formed by unconstrained vortex impingement upslope onto the bedrock surface toward the apex of the scallop. They vary in amplitude from barely discernible forms to features having a relief greater than 15 cm. Their dimensions rarely exceed 1.0 m–1.5 m horizontally. Coastal muschelbrüche inevitably develop first on steeper slopes and appear to grade upslope into sichelwanne, V-shaped grooves, and

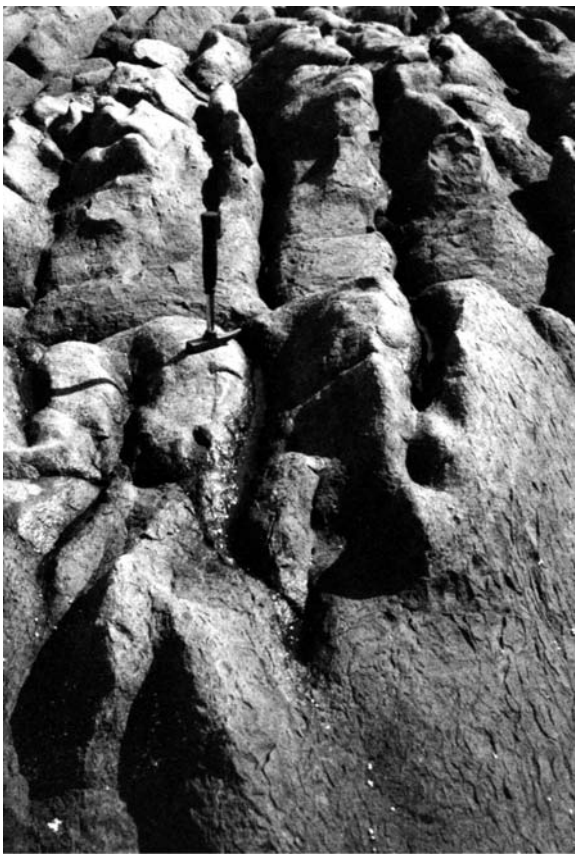

Figure 3.19. Sinuous grooves on a ramp at Tura Point, New South Wales, Australia.

flutes, as the vortices become more elongated and erosive. Sichelwanne have a more pronounced pedestal in the middle of the depression, while V-shaped grooves have a pointed rather than concave form downstream. V-shaped grooves have no sub-glacial equivalent and can span a large range of sizes. For instance, at Bass Point, New South Wales, V-shaped grooves approximately 10 m high and over 30 m wide have developed on slopes of more than 20°.

The term flute describes long linear forms that develop under unidirectional, high-velocity flow in the coastal environment. These are noticeable for their protrusion above, rather than their cutting below, bedrock surfaces (Figures 3.19 and 3.20). In a few instances, flutes taper downstream and are similar in shape to rock drumlins and rattails described for catastrophic flow in sub-glacial environments. In all cases, the steeper end faces the tsunami, while the spine is aligned parallel to the direction of tsunami flow. Flutes span a range of sizes, increasing in length to 30 m–50 m as slope decreases. However, their relief rarely exceeds 1 m–2 m. Larger features are called rock drumlins. The boulder trails at Tuross Head, mentioned above, are constrained

Figure 3.20. Flutes developed on the crest of a ramp 14 m above sea level at Tura Point, New South Wales, Australia. The depressions on the sides of the flutes are cavettos. Flow from left to right.

by flutes. Fluted topography always appears on the seaward crest of rocky promontories where velocities are highest. Flutes often have faceting or cavettos superimposed on their flanks. (Faceting consists of chiseled depressions with sharp intervening ridges.) They represent either the impingement of vortices instantaneously upon a bedrock surface or hydraulic hammering of rock surfaces by high-velocity impacts. Cavettos are curvilinear grooves eroded into steep or vertical faces by erosive vortices. While cavetto-like features can form due to chemical weathering in the coastal zone, especially in limestones, their presence on resistant bedrock at higher elevations above the zone of contemporary wave attack is one of the best indicators of high-velocity tsunami flow over a bedrock surface.

On flat surfaces, longitudinal vortices give way to vertical ones that can form hummocky topography and potholes (Figure 3.17). Potholes are one of the best features replicated at different scales by high-velocity tsunami flow. While large-scale forms can be up to 70 m in diameter, smaller features have dimensions of 4 m–5 m. The smaller potholes also tend to be broader, with a relief of less than 1 m. The smaller forms can exhibit a central plug, but this is rare (Figure 3.21). Instead, the potholes tend to develop as flat-floored, steep-walled rectangular depressions, usually within the zone of greatest turbulence. While bedrock jointing may control this shape, the potholes' origin as bedrock-sculptured features is unmistakable because the inner walls are inevitably undercut or imprinted with cavettos. In places where vortices

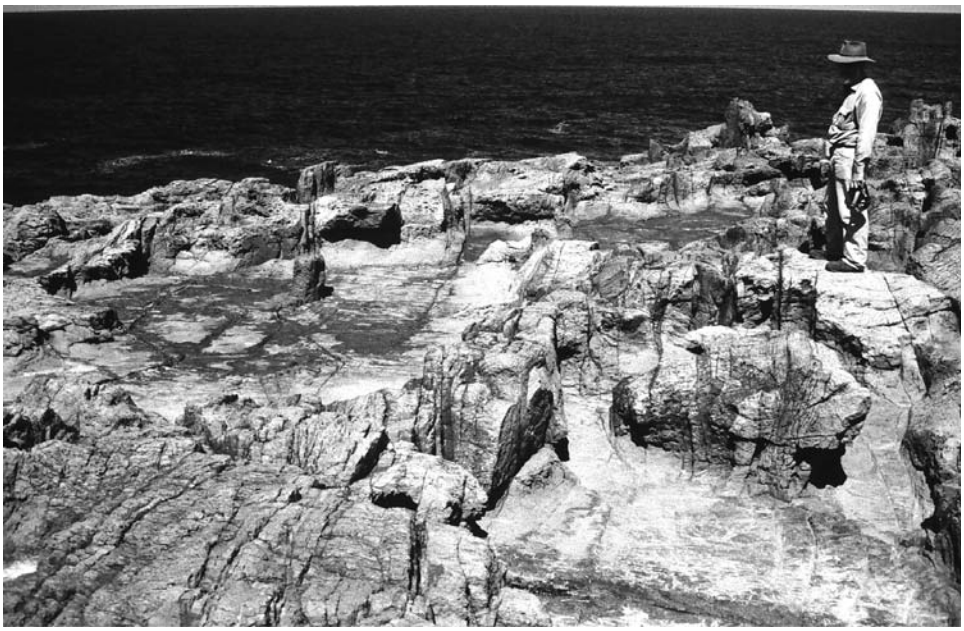

Figure 3.21. Small dissected potholes at the top of a 15 m high headland at Atcheson Rock, 60 km south of Sydney, Australia. The potholes lie on the ocean side of the canyon structure shown in Figure 3.23.

have eroded the connecting walls between potholes, a chaotic landscape of jutting bedrock with a relief of 1 m–2 m can be produced. This morphology—termed hummocky topography—forms where flow is unconstrained and turbulence is greatest. These areas occur where high-velocity water flow has changed direction suddenly, usually at the base of steep slopes or the seaward crest of headlands. The steep-sided, rounded, deep potholes found isolated on intertidal rock platforms, and attributed to mechanical abrasion under normal ocean wave action, could be catastrophically sculptured forms. Intriguingly, many of these latter features also evince undercutting and cavettos along their walls.

At the crests of headlands, flow can separate from the bedrock surface, forming a transverse roller vortex capable of eroding very smooth-sided, low, transverse troughs over 50 m in length and 10 m in width. Under optimum conditions, the bedrock surface is carved smooth and undular. In some cases, the troughs are difficult to discern because they have formed where flow was still highly turbulent after overwashing the crest of a headland. In these cases, the troughs are embedded in chaotic, hummocky topography. This is especially common on very low-angled slopes. Transverse troughs can also form on upflow slopes where the bed locally flattens or slopes downward. Under these circumstances, troughs are usually short, rarely exceeding 5 m. The smoothest and largest features develop on the crests of broad, undulating headlands.

Large-scale features

(Baker, 1978, 1981; Young and Bryant, 1992; Bryant and Young, 1996)

Large-scale features can usually be found sculptured or eroded on rock promontories, which protrude seaward onto the continental shelf. Such features require extreme run-up velocities that can only be produced by the higher or longer waves (mega-tsunami) generated by large submarine landslides or asteroid impacts in the ocean. One of the most common features of high-velocity overwashing is the stripping of joint blocks from the front of cliffs or platforms forming inclined surfaces or ramps (Figure 3.12). In many cases, this stripping is aided by the detachment of flow from surfaces, a process that generates enormous lift forces that can pluck joint-controlled rock slabs from the underlying bedrock. Where standing waves have formed, then bedrock plucking can remove two or three layers of bedrock from a restricted area, leaving a shallow, closed depression on the ramp surface devoid of rubble and unconnected to the open ocean (Figure 3.22). Ramps are obviously controlled structurally and have an unusual juxtaposition beginning in cliffs up to 30 m above sea level and sloping downflow often into a cliff. If these high velocities are channelized, erosion can produce linear canyon features 2 m–7 m deep and pool-and-cascade features incised into resistant bedrock on the lee side of steep headlands. These features are most prevalent on platforms raised 7 m–8 m above modern sea level. All features bear a resemblance to the larger canyon-and-cascade forms carved

Figure 3.22. The ramp at Bannisters Head on the New South Wales south coast. The tsunami wave approached from the bottom right-hand corner of the photograph. Erosion increases up the ramp that rises 16 m above sea level. The blocky boulders at the top of the ramp are over 4 m in diameter.

Figure 3.23. Canyon feature cut through the 20 m high headland at Atcheson Rock by a tsunami moving from bottom left to top right. Evidence exists in the cutting for subsequent downcutting of 2 m–4 m by a more recent tsunami. The latter event also draped a 0.5 m–2.0 m thick dump deposit over the headland to the right. This deposit has been radiocarbon-dated at around AD 1500. The small potholes in Figure 3.21 are located on the leftmost portion of the headland, while the large whirlpool shown in Figure 3.26 is located on the far side of the canyon.

in the channeled scabland of the western United States. Wave breaking may also leave a raised butte-like structure at the seaward edge of a headland, separated from the shoreline by an eroded depression. This feature looks similar to an inverted toothbrush (Figure 3.23). Large-scale fluting of a headland can also occur, and on smaller rock promontories, where the baseline for erosion terminates near mean sea level, the resulting form looks like the inverted keel of a sailboat. Often this form has a cockscomb peak produced by the rapid, random erosion of multiple vortices (Figure 3.24). While technically a sculpturing feature, the cockscomb looks as if it has been hydraulically hammered. On narrow promontories, vortices can create arches. While arches have been treated in the literature as products of chemical weathering or long-term wave attack along structure weaknesses, close investigation shows that many are formed by vortices. It is also possible for these horizontal vortices to form in the lee of stacks and erode promontories from their landward side (Figure 3.25).

Perhaps the most impressive features are whirlpools formed in bedrock on the sides of headlands. Whirlpools and smaller potholes commonly formed under catastrophic flow in the channeled scabland of Washington State. In coastal environments, whirlpools often contain a central plug of rock and show evidence of smaller vortices around their rim. Whirlpools can reach 50 m–70 m in diameter with central plugs protruding 2 m–3 m vertically upward from the floor of the pit at the quiescent center of the vortex. The best coastal example occurs on the south side of Atcheson Rock south of Bass Point, New South Wales (Figure 3.26). Here a large vortex,

Figure 3.24. Inverted keel-like forms at Cathedral Rocks, 90 km south of Sydney, Australia. Flow came from the right. The stacks formed between horizontal, helical (eggbeater) vortices. A sea cave is bored into the cliff downflow.

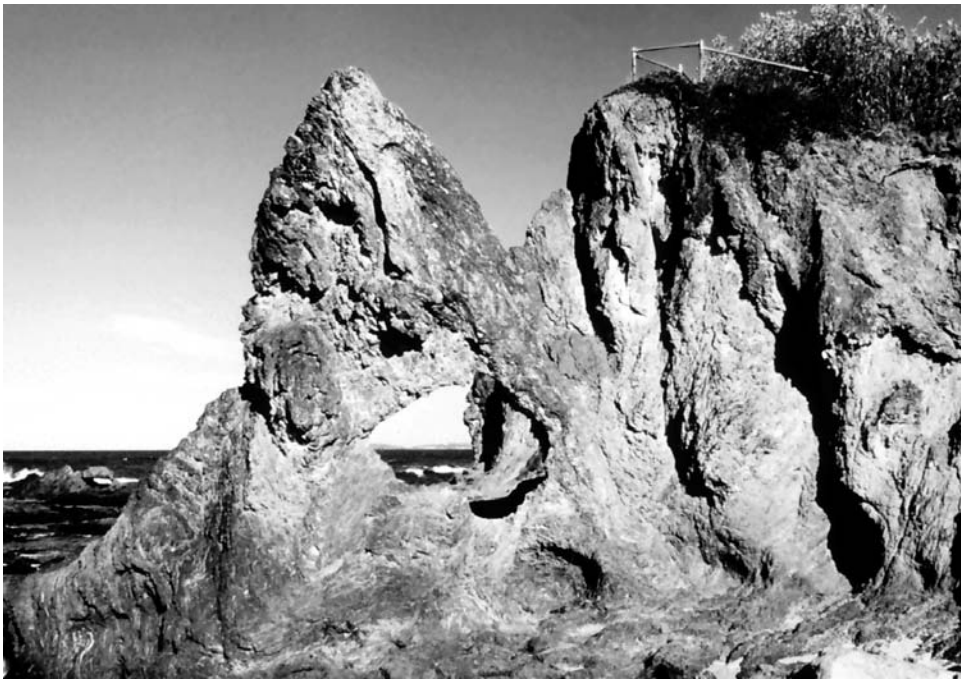

Figure 3.25. An arch at Narooma on the south coast of New South Wales, Australia. The tsunami wave swept towards the viewer along the platform in the background. A vortex on the seaward side eroded most of the arch. Joints in the rocks do not control the arch, nor does the rock face show evidence of major chemical weathering.

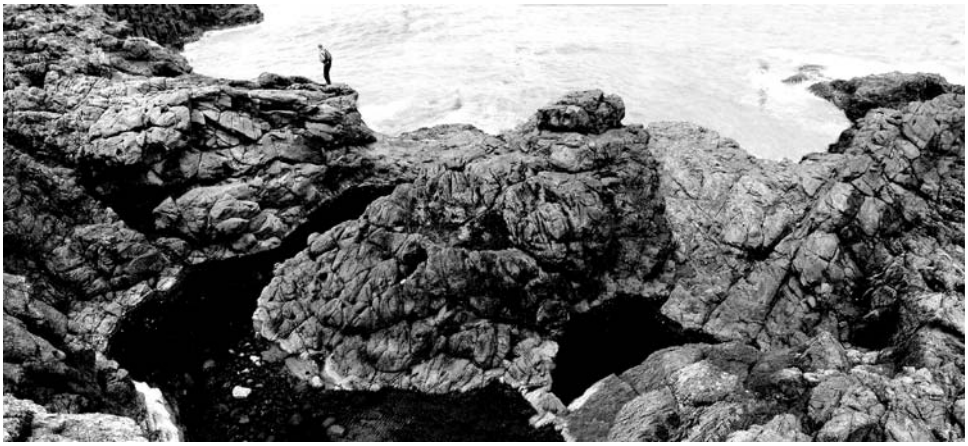

Figure 3.26. Whirlpool bored into bedrock on the south side of Atcheson Rock, New South Wales, Australia. The presence of drill holes and smaller potholes at the bottom indicates the existence of cavitation and multiple vortices, respectively. Helical flow operated in a counterclockwise direction around the central plug.

spinning in a counterclockwise direction, produced smaller vortices rotating around its edge on the upflow side of a headland. The overall whirlpool is 10 m wide and 8 m–9 m high. The central plug stands 5 m high and is surrounded by four 3-m diameter potholes, one of which bores another 3 m below the floor of the pit into resistant basalt. The counterclockwise rotation of the overall vortex produces downward-eroded helical spirals that undercut the sides of the pit, forming spiral benches. Circular or sickle-shaped holes were drilled, by cavitation, horizontally into the sides of the pothole and into the wall of the plug. Under exceptional circumstances, the whirlpool can be completely eroded, leaving only the plug behind. Figure 3.1 at the beginning of this chapter shows an example of this cut into aplite (granite) at Cape Woolamai on the south coast of Victoria, Australia.

Flow dynamics

(Alexander, 1932; Dahl, 1965; Wiegel, 1970; Fujita, 1971; Baker, 1978, 1981; Allen, 1984; Kor, Shaw, and Sharpe, 1991; Grazulis, 1993; Shaw, 1994; Bryant and Young, 1996)

Any model of the flow dynamics responsible for tsunami-sculptured bedrock terrain must be able to explain a range of features varying from sinuous cavitation marks several centimeters wide to whirlpools over 10 m in diameter. One of the controlling variables for the spatial distribution of these features is bed slope that can be higher than 10° at the front of promontories. Even a slight change in angle can initiate a change in sculptured form. For instance, sinuous cavitation marks can form quickly, simply by steepening slope by 1°–2°. Similarly, flutes can develop with the same increase in bed slope. This suggests that new vortex formation or flow disturbance through vortex stretching is required to initiate an organized pattern of flow vortices

able to sculpture bedrock. Because bedrock-sculpturing features rarely appear close to the edge of a platform or headland, vortices did not exist in the flow before the leading edge of the tsunami wave struck the coastline.

Bedrock-sculptured features are created by six flow phenomena: Mach–Stem waves, jetting, flow reattachment, vortex impingement, horseshoe or hairpin vortices, and multiple-vortex formation. Mach–Stem wave formation was described in Chapter 2. It occurs when waves travel obliquely along a cliff line. The wave height can increase at the boundary by a factor of 2-to-4 times. The process is insensitive to irregularities in the cliff face and is one of the mechanisms allowing tsunami waves to overtop cliffs up to 80 m high.

Tsunami, because of their long wavelength, behave like surging waves as they approach normal to a shoreline. Jetting is caused by the sudden interruption of the forward progress of a surging breaker by a rocky promontory. The immediate effect is twofold. First, there is a sudden increase in flow velocity as momentum is conserved and vortex formation is initiated. Second, the sudden velocity increase is sufficient for cavitation and creates lift forces that can pluck blocks of bedrock from the bed at the front of a platform. Equation (2.16) can be used to calculate theoretical velocities on some of the ramp surfaces. If the height of the tsunami wave is equivalent to the cliff-fronting ramps, then the calculated velocities can exceed $20\,\mathrm{m\,s^{-1}}$. These velocities are well in excess of the $10\,\mathrm{m\,s^{-1}}$ threshold required for cavitation.

The third phenomenon occurs if flow separates from the bed at the crest of a rocky promontory. This occurs at breaks of slope greater than 4°. Rock platforms overwashed by tsunami have changes in slope much greater than this. Some distance downstream, depending upon the velocity of the jet, water must reattach to the bed. Where it does, flow is turbulent and impingement on the bed is highly erosive. Standing waves may develop in the flow, leading to large vertical lift forces under crests. The bedrock plucking at the front of platforms and in the lee of crests is a product of this process.

S-forms spatially change their shape depending upon the degree of flow impingement and vortex orientation (Figure 3.27). In coastal environments, the flow by tsunami overwashing bedrock surfaces is not confined. The high velocity and sudden impact of the vortex on the bedrock surface causes the vortex to ricochet upward, and the unconfined nature of the flow permits the vortex to lose contact rapidly with the bed. This produces features that begin as shallow depressions, scour downflow, and then terminate suddenly leaving a form that is gouged into the bedrock surface with the steep rim downstream. Narrow longitudinal vortices impinging upon the bed at a low angle produce muschelbrüche that become sichelwannen and V-shaped grooves at higher angles of attack. Obstacles in the flow boundary layer form horseshoe vortices. As flow impinges upon an obstacle, higher pressures are generated that cause flow deflection and separation from the bed. This generates opposing, rotating vortices that wrap around the obstacle like a horseshoe or hairpin. The vortices scour into the bedrock surface downflow. Because these vortices lie within the boundary layer, they are subject to intense shearing by the overlying flow. This shearing fixes the vortices in position and keeps them straight. Horseshoe or hairpin vortices produce flutes that are progressively eroded into the

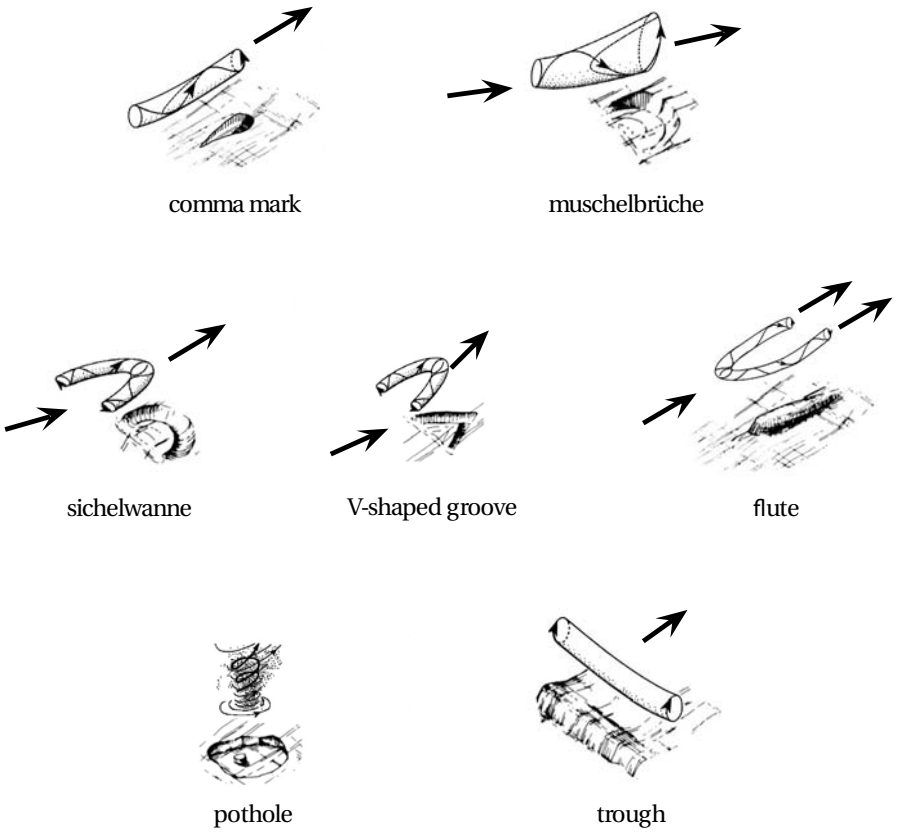

Figure 3.27. Types of vortices responsible for bedrock sculpturing by tsunami. Based on Kor, Shaw, and Sharpe (1991), and Shaw (1994).

face of platforms and headlands as long as high-velocity overwashing is maintained (Figure 3.20). At the largest scale the inverted keel-like stacks shown in Figure 3.24 formed between horizontal, helical (eggbeater) vortices. These helical vortices, besides eroding vertical stacks, have the capacity to bore caves into cliffs and form arches (Figure 3.25).

Multiple-vortex formation occurs at the largest scale and includes kolks and tornadic flow. Kolks are near-vertical vortices whose erosive power is aided by turbulent bursting. They are produced by intense energy dissipation in upward vortex action. The steep pressure gradients across the vortex produce enormous hydraulic lift forces. Kolks require a steep energy gradient and an irregular rough boundary to generate flow separation. These conditions are met when the tsunami waves first meet the steeper sides of headlands; however, the process does not account for the formation of whirlpools. Kolks may also be formed by macro-turbulence whereby eddies grow within larger rotational flow. This latter concept has been invoked to account for the formation of tornadoes and incorporated into a model of multiple-

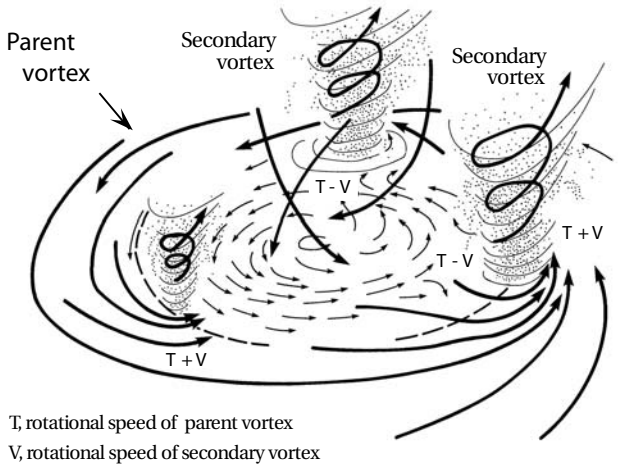

Figure 3.28. Model for multiple-vortex formation in bedrock whirlpools. Based on Fujita (1971), and Grazulis (1993).

vortex tornado formation that may be more appropriate in explaining the formation of whirlpools in tsunami-sculptured terrain.

Multiple-vortex tornadoes are produced by vortex breakdown within a tornado as air is pulled downward from above into the low pressure of the tornado. Smaller secondary vortices rotating in the same direction develop around the circumference of the larger parent vortex. Tsunami-generated whirlpools are formed by the vertical vortices embedded in flow overwashing a headland. These vortices expand and increase in rotational velocity with time. When the vortex is wide enough, water is pulled down into the center of the vortex and lifted upward at the circumference (Figure 3.28). When velocity is high enough, the vortex bores into bedrock and locks into position. Velocities exceed that necessary for cavitation as shown by the presence of drill marks in the whirlpool at Atcheson Rock (Figure 3.26). Toward the center of the vortex system, the directions of water movement in the mini-vortex and parent vortex are opposite and begin to cancel each other out. Here the resultant flow velocity is the rotational velocity of the parent vortex minus that of the mini-vortex. These lower rotational velocities aid the collapse of water into the center of the vortex, but at velocities that are too low to erode bedrock for part of the time. This process leaves a plug of bedrock in the middle of the whirlpool. Once multiple vortices form, the system of flow becomes self-perpetuating as long as there is flow of water to maintain the parent vortex. The fact that the plug height is always lower than the pothole walls suggests that multiple vortices develop in the waning stages of tsunami overwash after the crest of the tsunami has swept past and established the parent vortex.

Whirlpools form when flow velocities increase first through convergence of water over bedrock and then through funneling at preferred points along the coast. Critical rotational velocities required to erode resistant bedrock also take time to build up;

however, the flow under the crest of a tsunami wave is only sustained for a few minutes at most. Once a critical velocity is reached, bedrock erosion commences. The spin-up process causes vortex erosion to develop and terminate quickly, as is demonstrated by the fact that some potholes are only partially formed. Whirlpools, such as the one in Figure 3.26, are formed instantaneously in the space of minutes rather than by the cumulative effect of many wave events. Whereas mini-vortices in tornadoes can freely circumscribe paths around the wall of the tornado, those in whirlpools are constrained by the bedrock they are eroding.

This chapter has attempted to show that a myriad of distinct signatures produced by tsunami exist besides the descriptions of anomalous sediment layers that pervade the current literature. The most impressive of these additional signatures is produced by bedrock sculpturing. Most of the descriptions of individual signatures presented in this chapter indicate that they do not occur as isolated features but appear in combination with each other to form spatially organized suites that dominate some coastal landscape—such as rocky headlands. The description of these varied tsunami-generated landscapes constitutes the focus of Chapter 4.